Effect of Intermetallic Phases on the Tribological Behaviour of Iron and Aluminium Alloy

Saphalya Kumar Samantaray

Department of Metallurgical & Materials Engineering

National Institute of Technology, Rourkela

Effect of Intermetallic phases on the Tribological Behaviour of Iron and Aluminium Alloy

Dissertation submitted in partial fulfilment

of the requirement for the degree of

Master of Technology

in

Steel Technology

of

Mechanical Engineering Department

by

Saphalya Kumar Samantaray

(Roll No: 214MM2505)

Based on research carried out

Under the supervision of

Prof. Subash Chandra Mishra

May, 2016

Department of Metallurgical & Materials Engineering

National Institute of Technology, Rourkela

Department of Metallurgical & Materials Engineering

National Institute of Technology, Rourkela

May 26, 2016

Certificate of Examination

Roll Number: *214MM2505*

Name: *Saphalya Kumar Samantaray*

Title of dissertation: *Effect of Intermetallic Phases on The Tribological Behaviour of Iron and Aluminium Alloy*

We the below signed, after checking the dissertation mentioned above and the official record book (s) of the student, hereby state our approval of the dissertation submitted in partial fulfillment of the requirements of the degree of *Master of Technology* in *Mechanical Engineering* at *National Institute of Technology Rourkela*. We are satisfied with the volume, quality, correctness, and originality of the work.

Place: Prof. S.C. Mishra

Date: (Supervisior)

Dedicated To

My Family

Saphalya Kumar Samantaray

Declaration of Originality

I, Saphalya Kumar Samantaray, Roll Number 214MM2505 hereby declare that this dissertation entitled Effect of Intermetallic Phases on The Tribological Behaviour of Iron and Aluminium Alloy presents my original work carried out as a Master student of NIT Rourkela and, to the best of my knowledge, contains no material previously published or written by another person, nor any material presented by me for the award of any degree or diploma of NIT Rourkela or any other institution. Any contribution made to this research by others, with whom I have worked at NIT Rourkela or elsewhere, is explicitly acknowledged in the dissertation. Works of other authors cited in this dissertation have been duly acknowledged under the section "Reference" or "Bibliography". I have also submitted my original research records to the External Examiner for evaluation of my dissertation.

I am fully aware that in case of any non-compliance detected in future, the senate of NIT Rourkela may withdraw the degree awarded to me on the basis of the present dissertation.

May 26, 2016 *Saphalya Kumar Samantaray*

NIT Rourkela

Acknowledgement

I might want to express my profound feeling of appreciation and admiration to my supervisor cum Head of Department Metallurgical and Materials Engineering Prof. S.C. Mishra for his precious direction, inspiration, steady motivation or more just for his ever co-working state of mind that empowered me in raising this project in the present structure. I see myself as greatly fortunate to have the capacity to work under the direction of such a dynamic identity and for giving me important facilities in the department.

I might want to express my gratitude toward Sumanta Samal, Ashutosh Patnaik, Subrat Ku. Bhuyan and Ranjan Behera (Ph.D. Researchers, Department of Metallurgical and Materials Engineering), and my every companions with whose extra help in this study has been a succulent one.

My exceptionally extraordinary much gratitude goes to my parents and relatives. Their adoration, friendship and persistence made this work conceivable and the gifts and support of my dearest guardians enormously helped me in completing this exploration work.

CONTENTS

Abstract:

The Alloys based on Iron-Aluminium have important prospective for operational applications at elevated temperature because they maintain an outstanding elevated temperature corrosion resistance and they possess a lower density in compare with the other Iron - based materials such as stainless steels and cast iron. The cost of Ion-Aluminium based alloys has comparatively low because of the widely availability of their manufacturing and handling processes. Fe-Al alloy is acquiring its desirability in many business applications for its wear properties and corrosion properties, which is due to the presence of Aluminium as an alloying element.

The current study is focused on the investigation of the effect of the changes in phases due to heat treatment on the Tribological behavior of Fe-Al alloy. This experiment contains the analysis of microstructure by means of microscope, crystalline phases and its structure properties by means of X-Ray Diffraction analysis. Specimen were heat treated at different temperatures (600^{o}C, 750^{o}C, 950^{o}C, 1100^{o}C) and then followed by water quenching. The soaking time is being 1 hour. The analysis of microstructure, XRD and Vickers hardness test were done the post heat treatment process. Then the dry sliding wear behavior of the heat treated samples were done by the Ball-on-Plate tribometer. After that the SEM analysis of the worn surfaces were done. Then the samples were subjected to sea water and acid rain sample for the investigation of its corrosion resistance, that is for finding the phases which has corrosion resistance. SEM study of these corroded surface illustrated that the acid rain corroded samples showed some crack propagation on the surface that may be due to hydrogen and the sea water corroded sample shows deposition of cations present in sea water.

It has been found that the sample which was heat treated at 950^{o}C has highest hardness value in comparison with other samples as well as, it has the high resistance force against the indentation. And the material which was heat treated at 1100^{o}C has less hardness value but it is ductile and it may has resilience property. It has less resistance against the indentation. From the corrosion test we found the phase FeAl has showed the most resistance against corrosion from sea water and acid rain. We have also seen that there were changes in phases after the heat treatment in various temperatures.

Key Words: Iron-Aluminium alloy, Microstructure, Corrosion wear, Dry-sliding wear, XRD-Analysis

Index of Figures

List of Tables

CHAPTER - I

INTRODUCTION

1. Introduction:

1.1 Background of Iron- Aluminium alloy

Iron-Aluminium based alloys have significant prospective for operational application at elevated temperatures as they have an extraordinary elevated temperature corrosion resistance and they possess lower density examine in contrast to other iron- based materials. For example stainless steel and cast iron [1]. Fe-Al based alloys additionally offer equivalently low material expenses because of their manufacturing and handling are broadly accessible. In prospective their melting temperatures, which might be generally in range between 1200^{o}C to 1400^{o}C. Iron-Aluminium based alloys may be utilized for operational applications up to administration temperatures of 1000^{o}C. At high temperature strength and creep resistance are still missing so further alloy advancement is expected to enhance these properties [1,5].

1.2 Importance of aluminium in iron and steel as deoxidiser

Aluminium, as per a deoxidiser in steel entered the open-hearth and electric-furnace melt shop through the back door. For many years it was used surreptitiously as a corrective for over oxidized heats, and its use was therefore regarded as being an easy means of compensating for, and actually hiding, poor furnace practice. Although some high-quality steels are made without aluminium, this element is commonly used in controlling the deoxidation, and thus the quality of steels poured into ingots that are of the rimming, capped, semikilled, killed or fine-grain type. It is also used as a deoxidizer and to prevent pinhole porosity in steels that are poured into sand moulds [2].

The solid non-metallic inclusions present in all ferrous alloys are the inevitable consequence of the methods and equipment used for melting and refining these materials. Because many of these inclusions are of considerable size and differ appreciably in appearance from the background structure of a suitably polished and etched as soon as metallurgical microscope came into general use. The deoxidation with aluminium under carefully controlled conditions does not adversely affect the overall cleanliness of steel. Aluminium addition may cause a change in the type and size of inclusions, and it may consequently affect the inclusion rating as obtained by a microscope count of the number of readily visible inclusions in a definite section [3].

1.3 Importance of aluminium in iron and steel as alloying element:

With the simple and complex iron-aluminium alloys containing more than about 5% aluminium, difficulties in melting and processing increases as the aluminium increases, and special techniques (for example, induction melting) and the use of relatively high-purity raw materials are frequently necessary if poor surface, or an excess of aluminium oxide inclusions, or too high a carbon content is to be avoided. For the binary alloys, iron is melted in a basic-lined furnace and deoxidized with silicon or titanium; the slag is removed and the aluminium is then added. When the aluminium content exceeds 3 to 4% an oxide skin often forms around the pouring stream resulting in poor ingot or casting surface; but this can be avoided to some extent by the use of carbon and chlorine as a mold wash. Alloys containing less than 5% aluminium can be readily hot or cold worked; alloys with 5-16% aluminium can be hot worked if temperatures are carefully controlled, but are too brittle to be worked cold. Alloys containing more than 16% aluminium cannot be worked at all and used in the cast condition [4].

Aluminium greatly improves the heat resistance of iron and ferrous alloys generally. This increase is apparently due to the reduction by aluminium of any iron oxide formed at high temperatures, a process that will continue as long as the rate of diffusion of aluminium exceeds the rate of oxidation of the iron. The optimum amount of aluminium necessary to produce satisfactory scale resistance in relatively pure iron depends upon the temperature at which the material is heated; on an average, it should be at least 8% for temperature of 1650-2010^{o}F (900-1100^{o}C) and 10-13% for higher temperatures. In an essentially carbon free binary alloy of iron and aluminium, ductility as indicated by elongation and impact value is low if the aluminium exceeds 6% [5].

As an alloying element, aluminium strongly influences the microstructure and properties of cast iron. It also reduces the quantity of total carbon retainable in the alloy. When the aluminium content of cast iron is over 8%, the iron becomes progressively more scale resistance as the aluminium content is increased. The trans-former sheets made with 3.5% - 6.5% aluminium and 2%-3% manganese compare very favourably with silicon transformer alloys as far as their magnetic properties are concerned and are definitely superior in their capacity to be cold worked [6].

1.4 Objective of this investigation:

- Determination of the effect of changes in phases due to heat treatment on the tribological behaviour of iron aluminium alloy
- Determination of dry sliding wear behaviour of iron aluminium alloy
- Determination of corrosion resistance against acid rain and sea water of the iron aluminium alloy

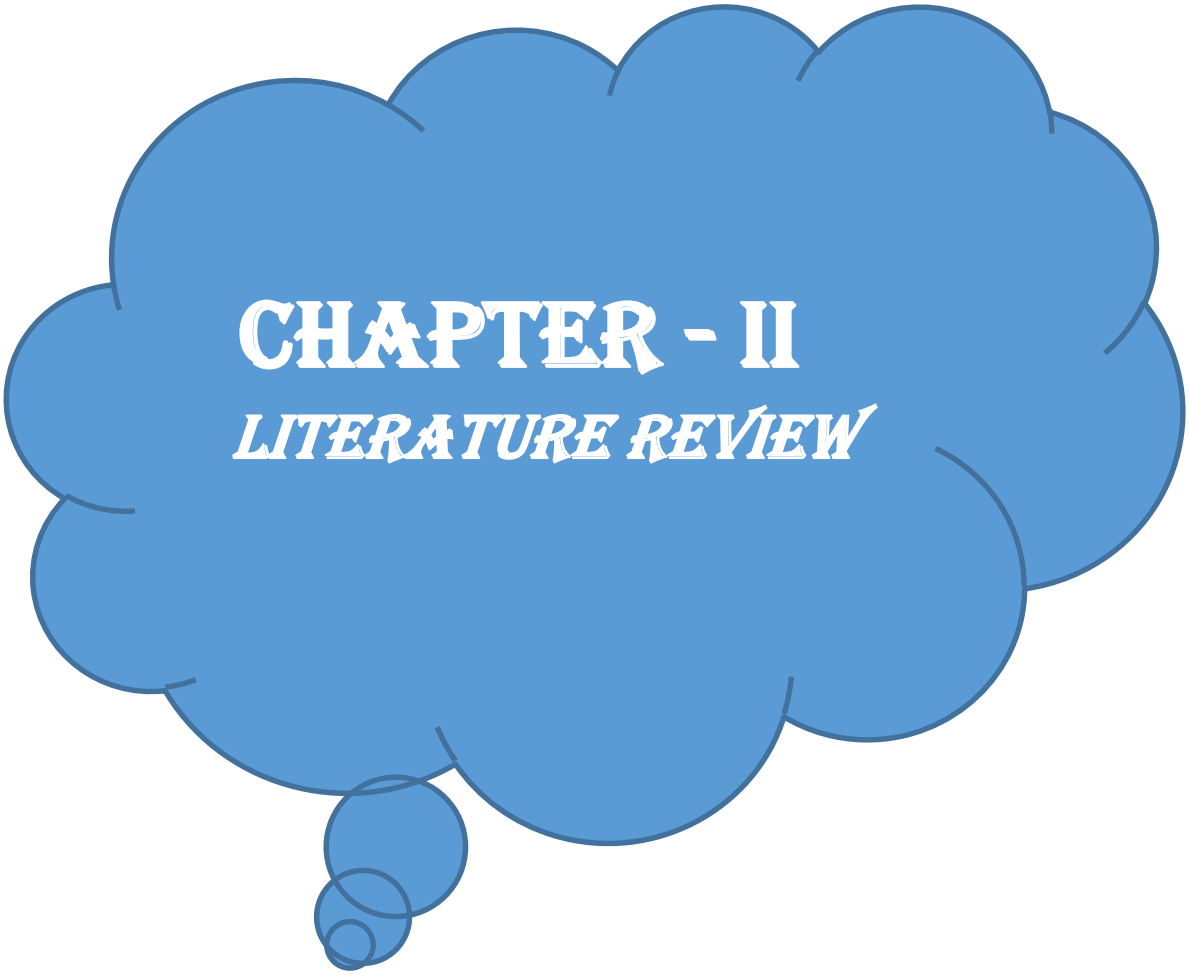

CHAPTER - II

LITERATURE REVIEW

2. Literature Review:

2.1 History of Iron:

Iron, which is an element (26 on the periodic table). The word '*iron'* comes from the Scandinavian word *iarn.* The chemical symbol '*Fe'* comes from the Latin word for iron, is *ferrum*. The French word for iron is *fer,* the German word, *Eisen.* And *ijzeret* is the Dutch word, and *hierro* is the Spanish *hierro*.

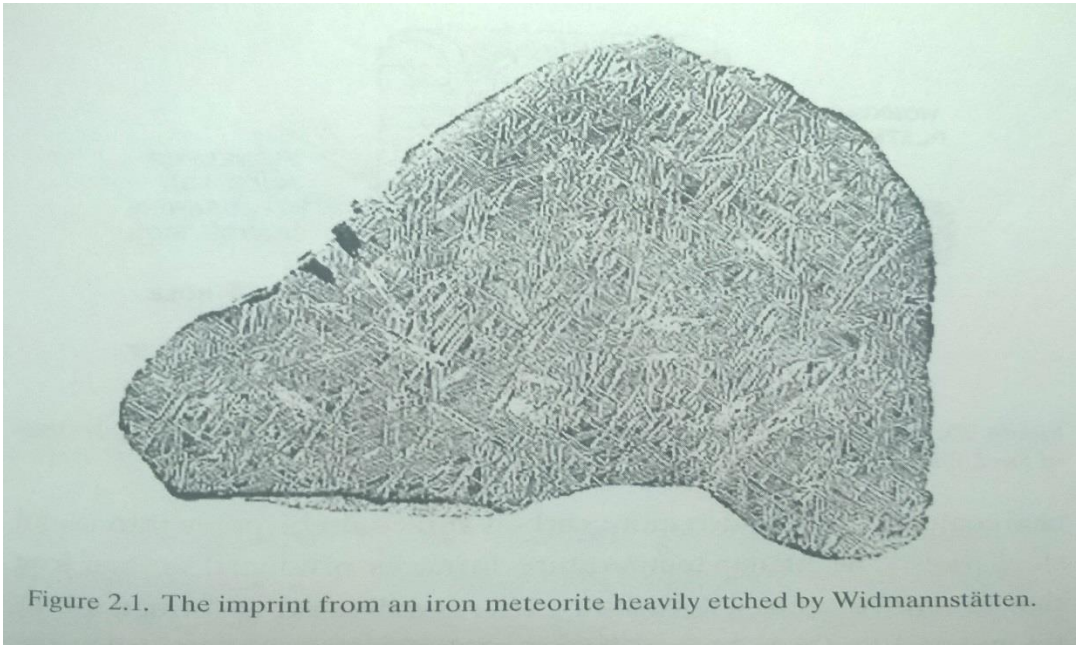

Figure 2.1. The imprint from an iron meteorite heavily etched by Widmannstätten.

The only sources of iron available to early humans were meteoric iron and native (*telluric*) iron. Both were scarce. Most meteorites are non-metallic; only about 65% are iron, and contained about 7 to 15% nickel. In 1808, William Thomson had sectioned, etched a meteorite and noted the remarkable patterns. Although he published his findings in 1808, these were attracted little interest. In 1808, an Austrian, Alois von Widmannstatten, also etched a meteorite and observed the structure and that is now known by his name. In 1820, widmannstatten and Carl von Schreibers published a book on meteorites, which contained a print from of a heavily etched meteorite (Figure 2.1). The native iron is even scarcer, being limited to small particles in western Greenland. Archaeological finds of iron with considerable amounts of nickel suggest that they were made from meteorites [7].

The first production of iron occurred dates back to at least 2000 BC in India and Sri Lanka. Thru 1200 BC, production of iron had been widespread in China and near the East. The most common iron ores are hematite (Fe_2O_3) and magnetite (Fe_3O_4). Smelting of iron involved heating iron ore (oxides of iron) with charcoal. The reaction of carbon with iron oxide produced carbon monoxide and carbon dioxide. The air was supplied by either a natural draft or by some means of blowing. The carbon content of iron produced in pit furnaces was usually low because of the low temperature achieved and resulted in semisolid sponge [8]

With shaft furnace, the higher temperature resulted in higher carbon content. In the furnaces, charcoal reacted with the air to form carbon monoxide, which was reduced some of the ore. The subsequent carbon dioxide reacted with charcoal to form more carbon monoxide.

The product of the lower-temperature furnaces were low in carbon and much like wrought iron. It was soft and formable. If heated in charcoal, it would absorb additional carbon and could be made into useful steel tools. The higher-temperature furnaces produced molten iron that contained up to 4% carbon. After it solidified, it formed a brittle material that was at first discarded. Later it was learned that the carbon content could be reduced by re-melting in contact with air. By 200BC, the Chinese had started casing the high-carbon material into useful objects.

There is a wrought-iron pillar in Delhi, India, that dates back to the late fourth century. It is more than 7 m in height and has resisted corrosion over the many centuries. Wrought iron is the principal material in the Eiffel Tower, constructed in 1887.

After about AD 1300, wrought iron was produced in a catalan furnace. The resulting semisolid product was pried out and hammered into bars. The American bioomery was a modification of this process, differing in that the charge of ore and charcoal were mixed together, and waterpower was used to create the blast [7,8].

2.2 History of Aluminium

Aluminium is an element (13 on the periodic table). The word *aluminium* comes from the Latin word *alumen.* English chemist, Sir Humphry Davy originally had called it alumimum in 1808, then amended this to *aluminum*, which remains the U.S word, but British editors further amended it to aluminium in 1812, the modern preferred British form to better harmonize with other metallic elements.

Alum, an aluminium based salt, was used extensively in ancient times. Commander Archelaus discovered that wood was practically flame resistance if it was treated using an alum solution; protected his wooden fortifications against flamed attack. Alum had been used throughout Europe from the XVI century onwards: in the leather industry, paper sizing and in medicine, i,e dermatology, cosmetology, stomatology and ophthalmology.

Hans Christian Oersted from Denmark had succeeded in 1825; however he had apparently produced an aluminium alloy with the elements used in the experiments, rather pure aluminium.

Hans Christians's work had continued by Friedrich Woehler, a German chemist, who had made a start working from 30 grams of aluminium powder in October 22,1827. It took another 18 years of continuous experimentation for Friedrich molten aluminium (globules) in 1845.

Henri-Etienne Sainte-Claire Deville an outstanding French chemist and technologist, ha transferred the chemical method of aluminium creation discovered by scientists to industrial application. He had improved the Woehler process and produced the first industrial aluminium together with his partners at the Charles and Alexandre Tissier's production facility in Rouen (France) in 1856.

The improvement of Aluminum had changed with the revelation of more cost-effective electrolytic strategy for generation in 1886. It was produced by Paul Heroult, a French architect and Charles Hall, an American understudy, autonomously at same time. The strategy included the lessening of liquid aluminum oxides in cryolite. This procedure showed incredible results, however required a colossal measure of electric force.

World war-II had changed the composition of the simple aluminum market bringing aviation and the manufacturing of the tanks and car motors to the bleeding edge. The war had pushed the nations for battling Germany to expand the utilization of their aluminum creation limits. Outlines of air ships were enhanced and the new aluminum composites were produced with them.

2.3 Phase diagram of Fe-Al alloy

The phase diagram of the iron-aluminium system is given in (Fig.1). From 0 to 38% (weight percentage) aluminium, the alloy forms a continuous series of solid solutions. In this field, order-disorder as well as magnetic to nonmagnetic transformations are known to exist. Since no phase changes are involved in these transformations, the boundaries have been shown

in the diagram as dashed and dotted lines. On the basis of terminology of Bradley and Taylor, the regions in the alpha field have been marked with subscripts; thus *m* and *n* indicates magnetic and nonmagnetic regions respectively; subscript 1, when prefixed to the *m* or *n*, indicates a region of ordered structure of the type Fe_3Al, and 2 indicates a region of ordered structure of type FeAl.

The iron-aluminium system has a closed gamma loop formed by the lowering of the A_4 and the raising of A_3 transformation temperatures. The gamma field extends to 1 or 1.2% aluminium. The aluminium content required to close the gamma loop probably depends, to some extent at least, on the purity of the alloy, particularly with respect to oxygen, carbon and probably nitrogen. According to Sykes and Evans, the change from the disordered to the ordered structure of the Fe_3Al (α_1) can be prevented for compositions of less than 13.9% aluminium by quenching from 1110°F (600°C), but not with higher aluminium contents.

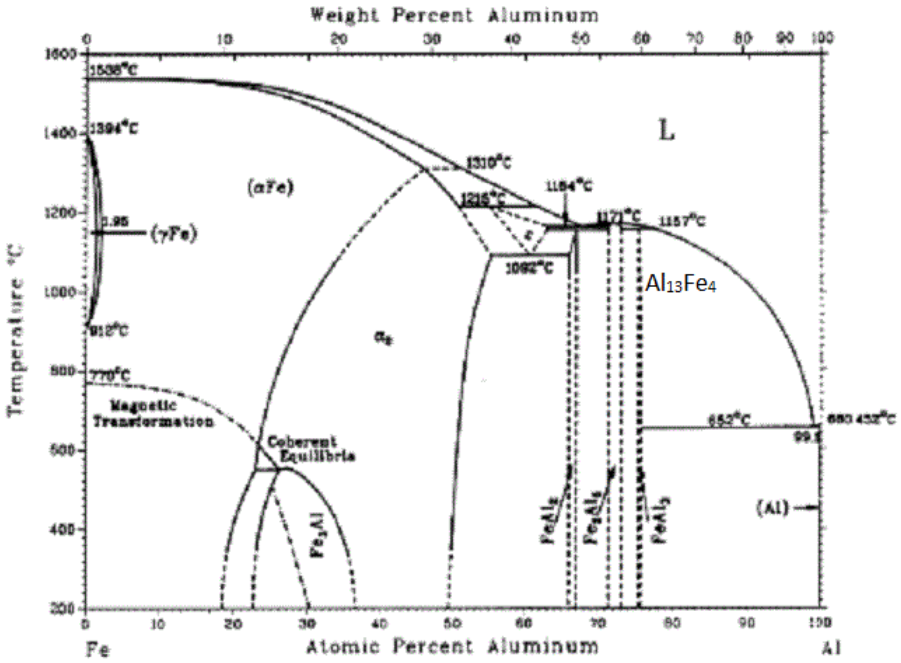

Fig. 2.2 Thermal equilibrium diagram of the iron-aluminium system, showing Phase fields of ordered and disordered alloys (A.Taylor & R.M.Jones)

Sykes and Bampfylde studied the properties of alpha solid solutions of iron-aluminium alloys and found that alloys containing from 0 to 5% aluminium are ductile and can be worked either hot or cold. Alloys containing from 5 to 16% aluminium are cold short and must,

therefore, be hot worked. Alloys containing more than 16% aluminium cannot be worked and must be ground.

Alloys outside the alpha-solid-solution field (containing more than 36% aluminium) are of no practical importance in ferrous metallurgy and will not be considered further in this monograph [9].

2.4 Historical origins of experimental in tribology:

Long before the initiation of historical records, Palaeolithic people experimented with a basic frictional phenomenon, the temperature rise in sliding contact. Sticks, stones and any other available materials were rubbed together to create sparks, sound and debris [10]. The Palaeolithic people then realized that the sparks generated might create that invaluable commodity, fire, which gave heat, light and protection from wild animals. Elementary methods of generating fire by banging two stones together were superseded by more advanced methods involving sliding surfaces which were probably developed by trial and error. The importance of high sliding speed was recognised by rotating the round end of a stick against another piece of wood, in order to create fire. To raise the sliding speed and frictional heat generated at the end of the stick still further, the string of a bow was threaded around the stick and the bow was pulled backwards and forwards to rotate the stick faster. Small splinters of wood or dried leaves were then placed around the rotating end of the stick. The leaves or wood fragments were known to catch fire when touching the hot surfaces of rotating contact. When added to build up a fire of useful size. Fire ignition by rotating stick is illustrated in Figure 2.3

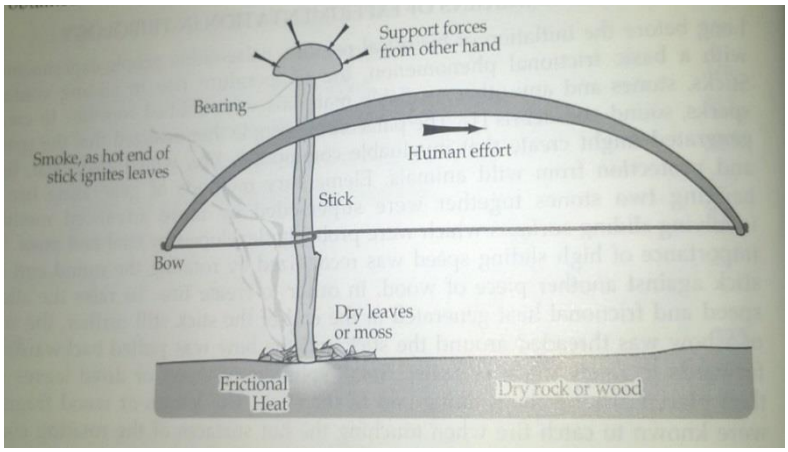

Figure 2.3: Palaeolithic Method of igniting a fire by using a rotating stick as an early example of tribological experimentation

The process of deduction that led to the rotating stick method to start a fire is unknown. Perhaps some adults observed children playing with sticks or perhaps they noted that hands warm up when rubbed together and then made a few tests of their own.

The pre-Christian history contains many other examples of the applied study of friction and wear, for example, the development of wheel or use of sledges and lubricants to move large masses for the construction of pyramids at Giza [10,11]. Although the development of a wheel is often heralded as the greatest invention in the human history it seems that the development of an axle with a set of bearings was a far greater and more practical invention. Contrary to the early progress of practical applications the scientific study of friction and wear in terms of abstract concepts and theories is far more recent. The earliest systematics studies of the laws of friction are ascribed to Leonardo da Vinci in the 16^{th} century [11]. Starting with a notion of force represented by weight and a test apparatus consisting of a smooth surface, some weights, cord and a pulley, da Vinci observed and recorded the amount of weights hanging by a cord that was required to move a block placed on the smooth surface. This experiment led to the deduction of the proportionality between friction force and weight of the block and the independence of friction force on contact area. These experiments were refined later by Amonton and Coulomb. It is important to realize that these early observation are merely the approximations to the modern view of frictional mechanics and that many complex phenomena between two interacting surfaces would have occurred in this apparently simple experiment. Similar experiments performed more recently have revealed the presence of micro-sliding when a frictional force insufficient to cause gross sliding is applied [12]. The basic principles of tribological experimentation are, however, best illustrated by da Vinci's experiments where a usefully simplified model of complex phenomena was obtained.

Tribology, like any other field of science, provides the researcher with only a limited number of concepts or models that can be tested with available experimental techniques. In friction and wear experiments the observed friction and wear phenomena are usually interpreted in terms of these concepts even though an incomplete interpretation results. Until now, most of the experimental studies were conducted on a macro scale aiming at explaining the tribological phenomena related to everyday engineering problems. Although satisfactory solutions were often found, the theoretical explanation provided was often wrong or not complete. Technological improvements to the experimental techniques have subsequently led to the gradual modification or change to the fundamental theories of friction and wear.

In recent years there was a great leap from macro to Nano scale observation resulting in the development of a new field of Nano tribology [13]. The new technologies developed allow the study of friction and wear processes at the fundamental level involving a single molecular contacts interface. The techniques include the surface force apparatus [14], the atomic force microscope (AFM) [15,16], the scanning tunnelling microscope [17,18], the quartz-crystal microbalance [19] and nonlinear optical techniques [20]. Among these new techniques the AFM is the most widely used. The operating principle of the AFM involves the traversal of a microscopic stylus across the surface of a specimen. The tip of the stylus is so fine that it can contact individual atoms on the specimen surface where quantum effects between the stylus and the specimen enable information about the nature of the surface atoms to be obtained. By measuring the forces on the stylus it is also possible to measure frictional force on an atomic scale. Localised force measurements of this nature have revealed that frictional forces vary considerably for even very small movements of stylus and that most surfaces have a heterogeneous classical tribological laws of friction are being modified or re-written as they are found not to be applicable on the atomic scale [19].

Recent development in computer technology allow to confirm and explain many experimental observations and also to advance theoretical calculations of complex phenomena occurring within the tribological interface. One such an area where computer modelling is widely employed is molecular-dynamics (MD) simulation [21].

2.5 Previous Research:

Outstanding high-temperature quality and erosion resistance of an iron-aluminum compound have been of interests for use in basic applications [22]. Specifically, the mechanical properties of steels containing iron and aluminum can be taken care of by the variety in the rate of aluminum, sort of warmth treatment, and grain size creating certain materials to be engaged to particular mechanical – metallurgical prerequisites as an element of the parameters [23].

Frangini and associates have investigated on the consumption conduct of Fe-Al amalgam in a fluid situation by an electrochemical investigation joined with XPS. Aluminum expansion to press enhances the capacity to shape a defensive uninvolved film in H2SO4 arrangement and the passivating layer of iron and aluminum oxides is owing to the consumption resistance [24,25]. Schaepers and Strehblow have explored the passive layers of the Fe-Al compounds in acidic and soluble electrolytes, and presumed that aluminum

expansion to press diminishes the separation current thickness and increments the relative part of aluminum oxide with a most extreme inside the inactive layer [26].

Guan et al. [27] dissected the wear conduct of a Fe-28Al-10Ti combination in a ball-on-plate tribometer utilizing alumina as the counter body material; tailing this same sort of wear examination, Zhang et al. [28] tried a sintered example of Fe-28Al-3Cr combination utilizing against a Si4N3 circle as counter body material. In addition, Sharma et al. [29] considered the tribological conduct of Fe-28Al-3Cr compound utilizing a ball-on-plate hardware arrangement with a tungsten carbide circle as the counter body material, and Kim and Kim [30] reported aftereffects of the sliding wear conduct of Fe-25Al, Fe-28Al examples materials in a pin-on-plate wear test strategy, utilizing AISI 52100 bearing steel as the counter body material.

A few analysts examined that impact of aluminum on the plastic disfigurement and work solidifying rate of Hadfield steel. They demonstrated that Al can enhance the yield quality [31, 32]. Zuidema and Subramanyam [33] presented the Al expansion on the work solidifying wear resistance. Their outcomes on the rough wear conduct were not finished. Notwithstanding, they clarified the stacking deficiency vitality and element strain maturing parts on the malleable properties of Hadfield steel.

Jiangwei Ren and Dong Li showed that grain refinement leads to the strengthening of Fe_3Al alloy by Surface Mechanical Attrition technology. They controlled the grain refinement of Fe_3Al by dynamically recrystallization mechanism under the condition of severe plastic deformation. The peak micro hardness of Fe_3Al alloy increases 12% after 5min of surface mechanical attrition technology[34].

G. Hasemann, J.H Schneibel, M. Kruger, E.P George demonstrated the impact of warmth treatment on the room temperature yield anxiety of expelled and recrystallized Fe3Al compounds with aluminum focuses running from 23.5 to 32 at% has been inspected. For aluminum fixations somewhere around 28 and 32 at% and toughening/extinguishing temperatures somewhere around 400oC and 900oC, the deliberate yield anxiety are reliable with reported estimations of warm opportunity focuses and opening movement rates. Since Fe3Al may possibly be reinforced by a few instruments, it is not clear climate opening fortifying is the main component in charge of the watched toughening and extinguishing impacts. However as an aftereffect of this work those other fortifying instruments might be inspected all the more indisputably by planning heat medications for which the opportunity

compressions and along these lines the opening reinforcing component might be disconnected from the opening reinforcing [35].

Dry sliding wear conduct of different Fe3Al requested intermetallic amalgams had been examined by different specialists. Garima Sharma and M. Sundaraman demonstrated that wear rates of aluminides (Fe-28at%Al-3%Cr) diminishes with an expansion in sliding separation and expansions with an increment in typical burden by ball on spot machine [36]. Their further dry sliding by Pin on plate examination on iron aluminide (Fe-28Al, Fe-28Al-3Cr, Fe-28Al-5Cr) demonstrated that the wear rate expanded with the expansion of typical connected load and sliding pace, wear resistance of the aluminides expanded with expansion in chromium content [36]. Yong-Suk Kim and Yong-Hwan Kim researched in iron aluminide by shifting the aluminum weight rate (25, 28, 30at%Al) and demonstrated that wear rate expanded with the expansion in connected ordinary load and sliding separation, wear resistance of aluminides diminished with the expansion in aluminum substance [37].

CHAPTER - III

EXPERIMENTAL DETAILS

3. Experimental Details:

3.1 Flow chart of this investigation:

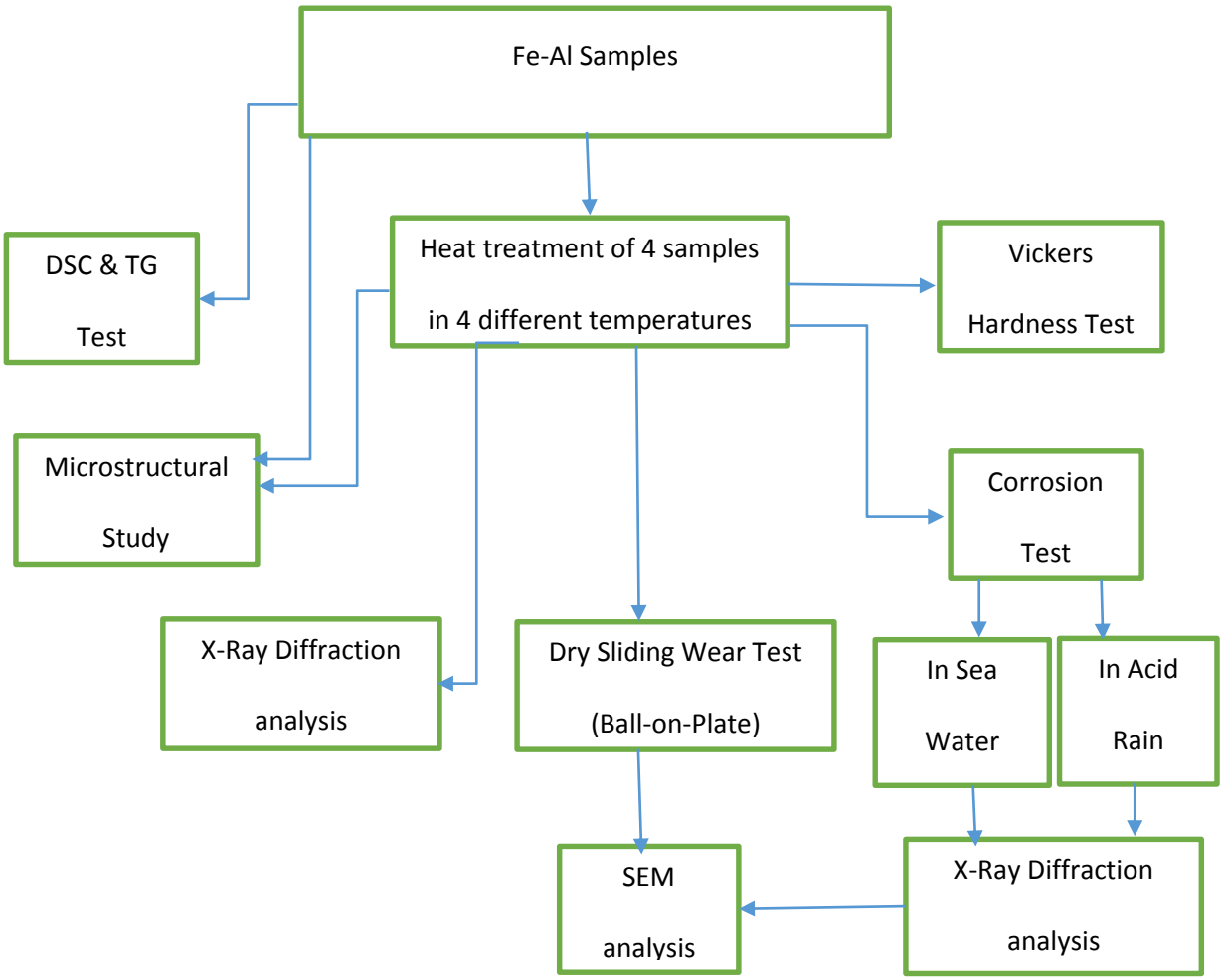

3.2 Experimental Procedure:

3.2.1 Sample Preparation:

Iron and (5%) Aluminium was melted in an induction furnace and the crucible was casted in graphite mould. Then the cast ingots are hot rolled to sheet form. Five samples having dimension (5*3*0.5) cm were cut from that hot rolled sheet.

3.2.2 DSC and TG:

DSC – Differential Scanning Calorimetry – measure separately, the temperature contrast and the warmth stream distinction between an example and a reference material subjected to same temperature variety in a controlled air. DSC decides the temperature and warmth of change. Properties measured by DSC incorporates stage changes, glass move, dissolving, immaculateness, vanishing, sublimation, Heat limit and so on. Thermo Gravimetry measures weight changes in a material subjected to temperature variety in a controlled environment. Properties measured by TG incorporates oxidation, decrease, hydration, drying out, assimilation and so on.

The hot moved Fe-Al alloyed example was cleaned to make its surface level. And after that slice to the measurement of 3*3*3 mm for the DSC and TG examination in encompassing climatic condition and having temperature range 50oC to 1200oC.

3.2.3 Heat treatment:

The four samples, the hot rolled Fe-Al alloys were taken and exposed to muffle furnace for heat treatment. For sensitization operation the Fe-Al alloys samples were subjected to different temperatures, 600^{o}C, 750^{o}C, 950^{o}C and 1100^{o}C for 1 hour for soaking in same muffle furnace followed by water quenching.

3.2.4 X-Ray Diffraction Analysis:

For the identification of the different crystalline phases which were existing in the specimen X-Ray diffraction technique is used. The XRD analysis was done in Ni-filtered Cu-Kα radiation Philips X-Ray Diffractometer. The XRD was performed at 30 KV and 20 mA using a Cu- Kα target diffract meter. The Scanning of these samples were done in angular range 2θ from 10° to 90° at a scanning speed of 5°/min. The all possible characteristic values

of brag angle, d-spacing and intensity from JCPDS cards were compared with d-values obtained from XRD patterns to identify the various X-ray peaks obtained.

3.2.5 Metallography Study:

The specimens were placed on a belt grinder for initial polishing for the purpose of microstructure study. Specimen were moved front and back during the grinding through the surface of the flat belt grinder. During grinding operation, water was used as a coolant. Materials were dipped inside the water time to time throughout the grinding operation. After completion of belt grinding samples were polished by a series of emery papers. It contains subsequently better grains, for example, evaluations of 1/0, 2/0 and 3/0. The specimen were moved in opposite heading to the current scratches amid every cleaning operation. In the wake of cleaning with the emery papers the specimens were cleaned by utilizing a turning wheel secured with exceptional sort of material. The fabric was accused of fine aluminum grating and water. At last the specimens were cleaned by jewel cleaning. In the wake of cleaning tests were painstakingly cleaned with cleanser water, and accordingly dried utilizing a drier. The examples were then scratched with newly arranged etchant Nital (80ml ethanol, 20ml HNO3) for infinitesimal examination.

3.2.6 Vickers Hardness Test:

In metallurgy, Hardness is characterized as the capacity of a material to oppose plastic disfigurement. As per the word reference of metallurgy hardness is the resistance of a material to space. This is the standard sort of hardness test where a pointed or adjusted indenter is squeezed into a surface under a generously static burden.

Vickers Hardness Test is the standard technique for measuring the hardness of metals, especially those having hard surface. The surface is subjected to standard weight for a standard time allotment by method for a pyramid-formed precious stone. The slanting of the subsequent space is measured under a magnifying instrument and Vickers hardness esteem read from a change table.

The warmth treated specimens were cleaned by emery papers of particular coarseness size for hardness estimation. Vickers hardness test was performed at room temperature to measure the hardness of Fe-Al alloyed example. The heap was connected was connected by the precious stone indenter for 10 seconds amid testing of all the warmth treated example. Twenty perusing are taken out of ten perusing are taken on a level plane and another ten readings were taken vertically and found the normal quality to get the last hardness number.

3.2.7 Dry sliding wear test:

Here Ball-on-plate wear machine is used for our dry sliding wear test. Careful preparation of test sample is an essential part of experimental methodology. Materials were cut into the squared shaped having dimensions of 18*18 mm. Then polishing had been done to make the surface flat as well as smooth for SEM analysis purpose. Then the samples were rinsed with alcohol and dried before the experiments. Here diamond indenter is used against our heat treated Fe-Al alloyed specimen.

3.2.8 Scanning Electron Microscopy Analysis:

A Scanning Electron Microscope (SEM) is a type of electron microscope that produces images of a sample by scanning it with a focused beam of electrons. The electrons interact with the atoms in the sample, producing various signals that contain information about the sample's surface topography and composition.

The worn surfaces of the different heat treated samples were examined under SEM and images were taken from which wear track, mechanism of wear and material type has been investigated.

3.2.9 Corrosion Sample Preparation:

The heat treated samples were subjected to corrosion test in Acid rain sample and Sea water. The sea water was collected from the Bay-of-Bengal. The following table shows the composition of the sea water.

Table 1: Contains the composition of sea water

Major elements present in sea water of 34.5 ppt salinity, their ionic forms and their levels

Type of ion	Element	Concentration (mg/litre)	% by weight
Cations	Sodium (Na^+)	10500	30.42
	Magnesium (Mg^{2+})	1350	3.91
	Calcium (Ca^{2+})	400	1.16
	Potassium (K^+)	380	1.10
	Strontium (Sr^{2+})	8	0.02
Anions	Chloride (Cl^-)	19000	55.04
	Sulphate (SO_4^{2-})	2655	7.04
	Carbonate (CO_3^{2-})	140	0.41
	Bromide (Br^-)	65	0.19
	Borate (BO_3^{3-})	20	0.06
	Silicate (SiO_3^{2-})	8	0.02
	Fluoride (F^-)	1	0.003

The Acid rain sample was made in the laboratory with PH 3, which is the most common PH for actual acid rain. The methodology of the preparation of the acid rain sample is given below.

$$S_{(s)} + O_{2(g)} \rightarrow SO_{2(g)}$$

$$SO_{2(g)} + H_2O_{(l)} \rightarrow H_2SO_{3(aq.)}$$

Drops of bromothymol blue solution was added to distilled water in a glass jar until the water becomes a light blue colour. In presence of an acid bromothymol blue will turn yellow. Then solid sulphur was burned with the help of gas lighter and this burned sulphur was kept inside with a holder and the lid of the jar was covered. This arrangement was kept as it is, till white fume from the burned sulphur completely mixed with the water. Then the covered glass jar was shaken well and intensity of the yellow colour was measured with a PH meter.

CHAPTER - IV

RESULT & DISCUSSION

4. Results and Discussion:

4.1DSC & TG:

These experiments are done to find the reactions taking place at different temperatures. From DSC vs Temperature graph (figure 4.1 a & b), some downward peaks are clearly visible in the range starting from 600^{o}C to 1100^{o}C. Hence I selected four temperature for heat treatment purpose. These temperatures are 600^{o}C, 750^{o}C, 950^{o}C and 1100^{o}C. From TG vs Temperature graph, it can be interpreted that there is sudden increase in mass after 1150^{o}C. This is may be due to the starting of oxidation reaction.

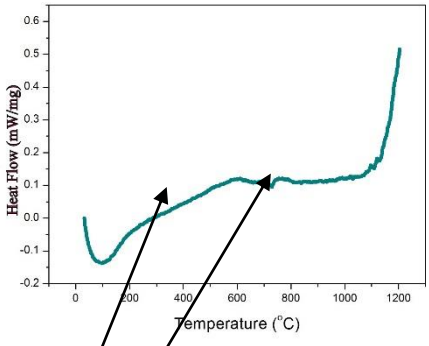

Fig 4.1(a): DSC curve of pre heat treated hot rolled sample

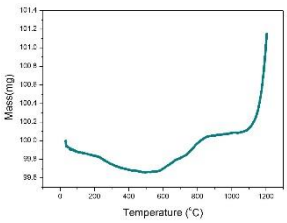

Fig 4.1(b): TG curve of pre heat treated hot rolled sample

4.2 Microstructural Study:

4.2.1 Microstructure of the hot rolled sample before heat treatment

The figure 4.2(a) illustrates the optical micrograph of investigate pre heat treated hot rolled Fe-Al alloy which illustration shows a polygonal grain structure. The black dots present in the microstructure figure are graphite due to carbon present in the Fe-Al alloy. When aluminium is added to liquid iron will reduce the iron oxide to metallic iron. Further it will also reduce CO or CO_2 gases to free carbon and subsequently degasify, calm the bath and avoid blowholes amid solidification and cooling.

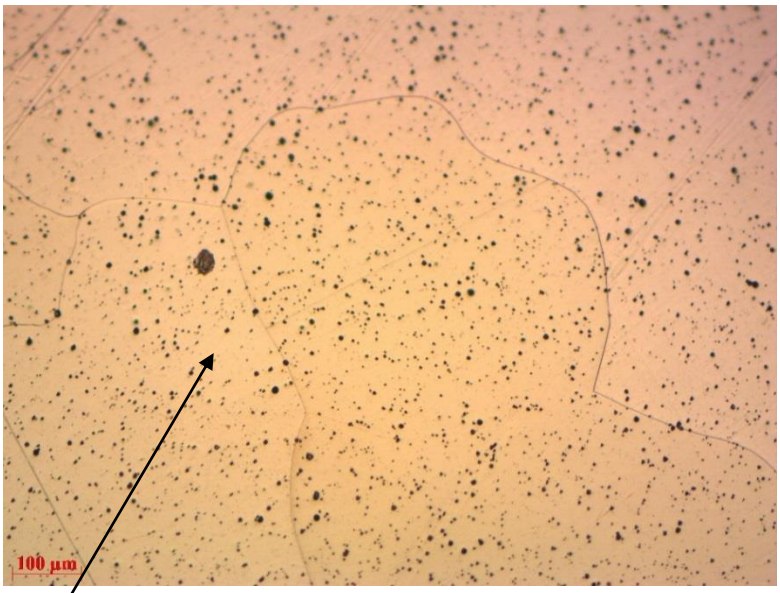

Fig 4.2(a): Microstructure of pre heat treated hot rolled sample

Small dots may be due to the presence of carbon

4.2.2 Microstructure of Heat Treated Samples:

From the figure 4.2(d) it is watched that the reliably circulated pole – like k-stage Fe3AlC1 is available in the grain limit. This k-stage gives quality to the Fe–Al amalgams with Al substance up to around 50 at.% which comprises in the sythesis scope of B.C.C disarranged Fe–Al composites, DO3 - requested Fe3Al compounds and B2-requested Fe-Al combinations. K-stage is essentially ferromagnetic requested structure of Fe3AlCX. K-stage is not seen obviously from the microstructure of pre warmth treated example. Since before warmth treatment k-stage is fine. The impact of warmth treatment towards microstructure and stage change uncovers from (figure 4.2 b, c, d and e). The microstructure of tests after warmth treatment are essentially coarsened, because of coarsening of microstructure, pole like K-stage Fe3AlCX hastens has additionally be coarsened. The span of K-stage Fe3AlCX accelerates has expanded. Such quick coarsening energy of K-stage Fe3AlCx precipitation happens due the high diffusivity of the interstitial carbon in the Fe3Al framework and the way that for the development of the k-stage Fe3AlCx, the dispersion of carbon is required. It can be expressed

that the performed heat treatment was adverse to both—the room-temperature flexibility and the high-temperature quality of all researched compounds because of the watched coarsening of microstructures. There is an emotional change in the microstructure of extinguished from 1200oC example as appeared in figure 4.2 (d) ,the measure of graphite (dark spots in miniaturized scale structure) is nearly low. May be, the carbon has joined with the iron and aluminum, unless it is accelerated in such finely separated state that it is imperceptible under the amplification utilized.

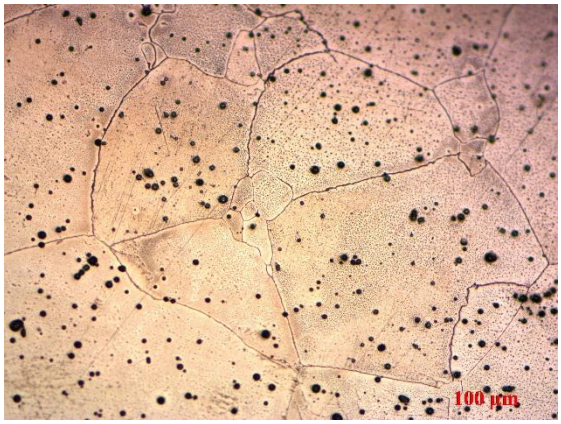

Fig 4.2(b) microstructure after heat treatment at at (600ºC)

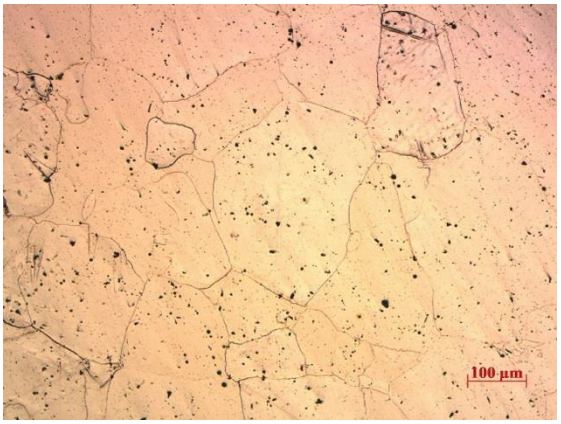

Fig 4.2(c) microstructure after heat treatment at (750ºC)

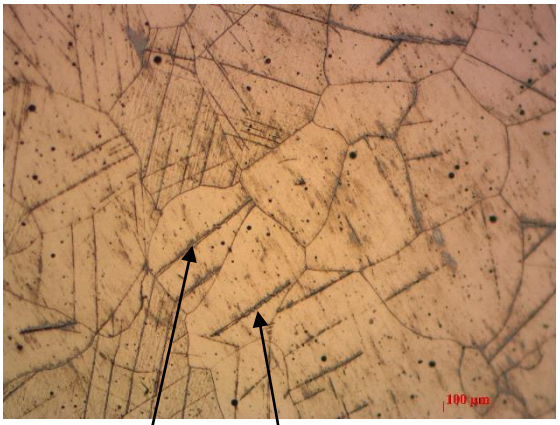

Fig 4.2(d) microstructure after heat treatment at (950ºC)

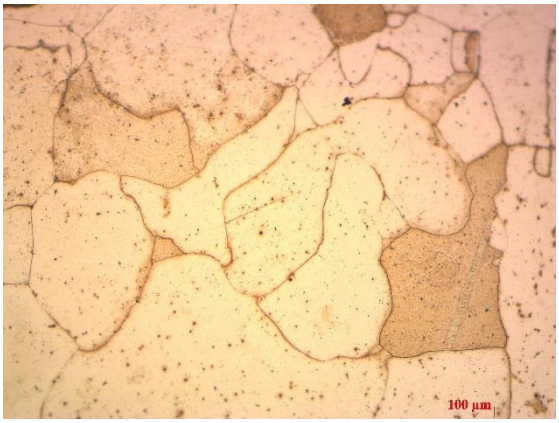

Fig 4.2(e) microstructure after heat treatment at (1100ºC)

Rod like k-phase Fe3AlCx

4.3 XRD Analysis:

4.3.1 XRD analysis of hot rolled sample before heat treatment:

From the figure 4.3(a) it is observed that the pre heat treated hot rolled Fe-Al alloy has (0 1 1), (2 0 0), (1 1 2) and (0 6 0) planes. This shows indication towards the bcc structure. The

sharp peak obtained in the diffraction pattern justifies the highly ordered structure of alpha phase. It is noted that by XRD-analysis, only α ferrite phase is present, but k-phase is not present.

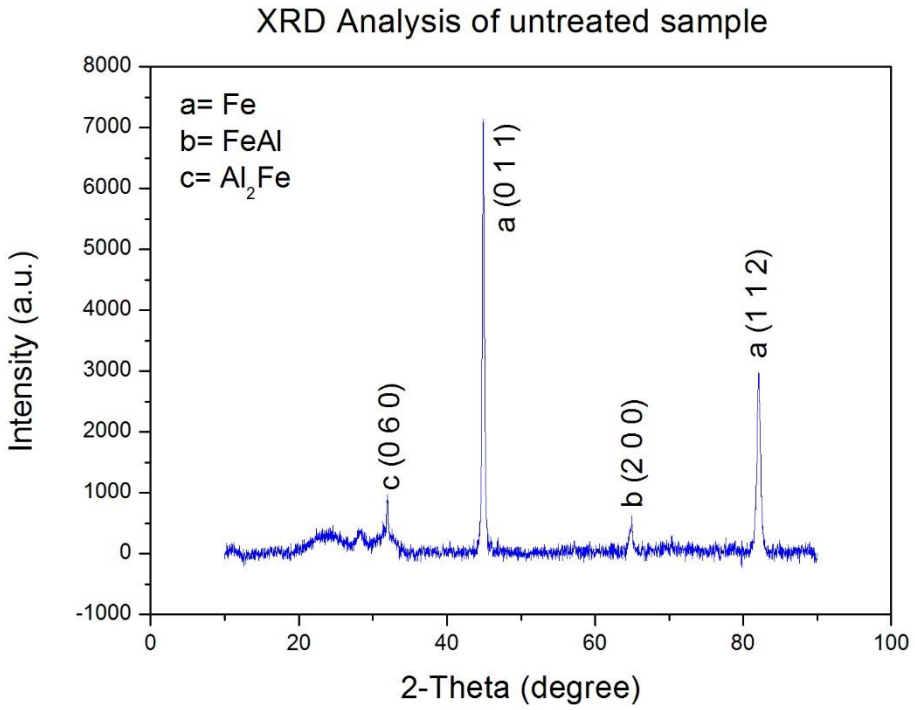

Fig 4.3(a): X-Ray Diffraction analysis of pre heat treated hot rolled sample

4.3.2 XRD analysis of heat treat sample:

The influence of heat treatment towards the phase transformations reveals from figure 4.3 (b). The peak position and integrated intensities of Fe-Al alloy after heat treatment in different planes. Which indicates that it gives bcc structure for all heat treated sample. It is assumed that the area under the integrated intensity of each peak to be proportional to the quantity of material present. The XRD pattern of heat treated sample shows the presence of different phase such as Fe, Al and a new phases like C_3Fe_7, $C_1Al_1Fe_3$, Al_3Fe etc. It is important to note that, XRD pattern of quenching from 950^oC sample reveals a new phases C_3Fe_7, $C_1Al_1Fe_3$ with higher intensity. This new phase improves the hardness.

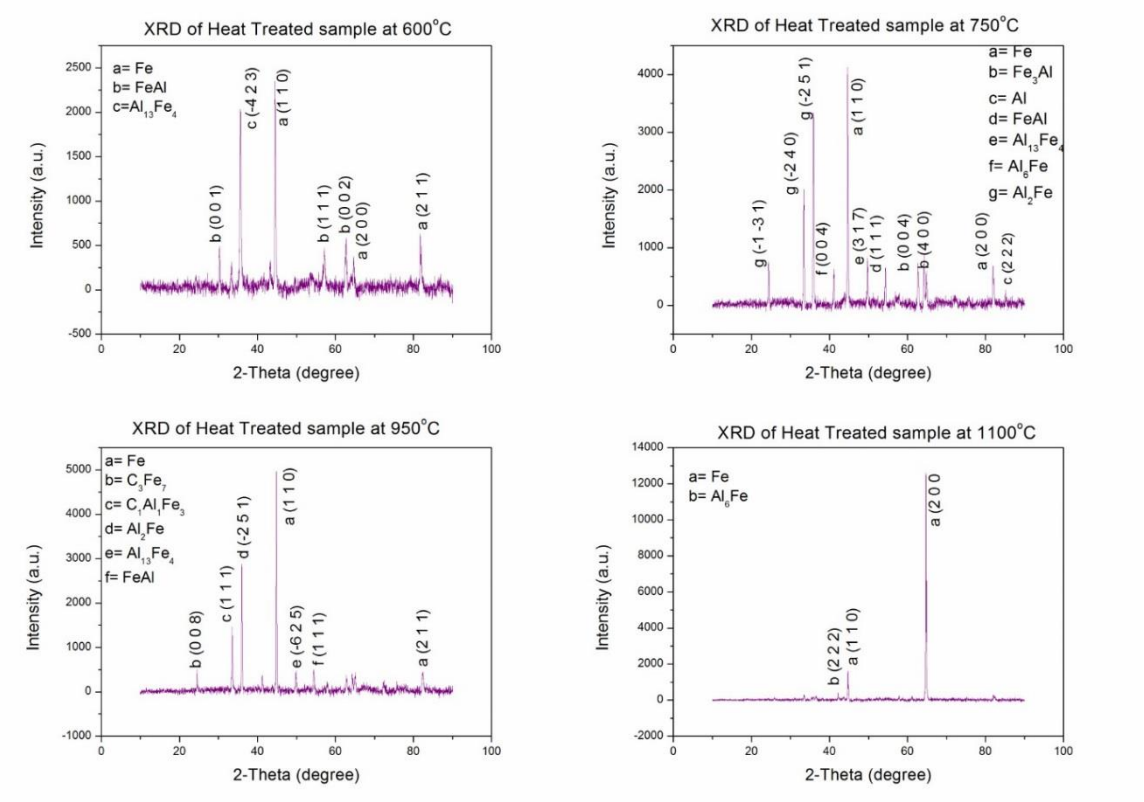

Fig 4.3(b): X-Ray Diffraction analysis of post heat treated hot rolled Fe-Al alloy sample

4.3.3 XRD analysis of Acid rain sample:

Table 2: Description of the samples name that were used in acid rain treatment

Sample Name	Description of Sample
A-5	Heat Treated at 600°C
A-6	Heat Treated at 750°C
A-7	Heat Treated at 950°C
A-8	Heat Treated at 1100°C

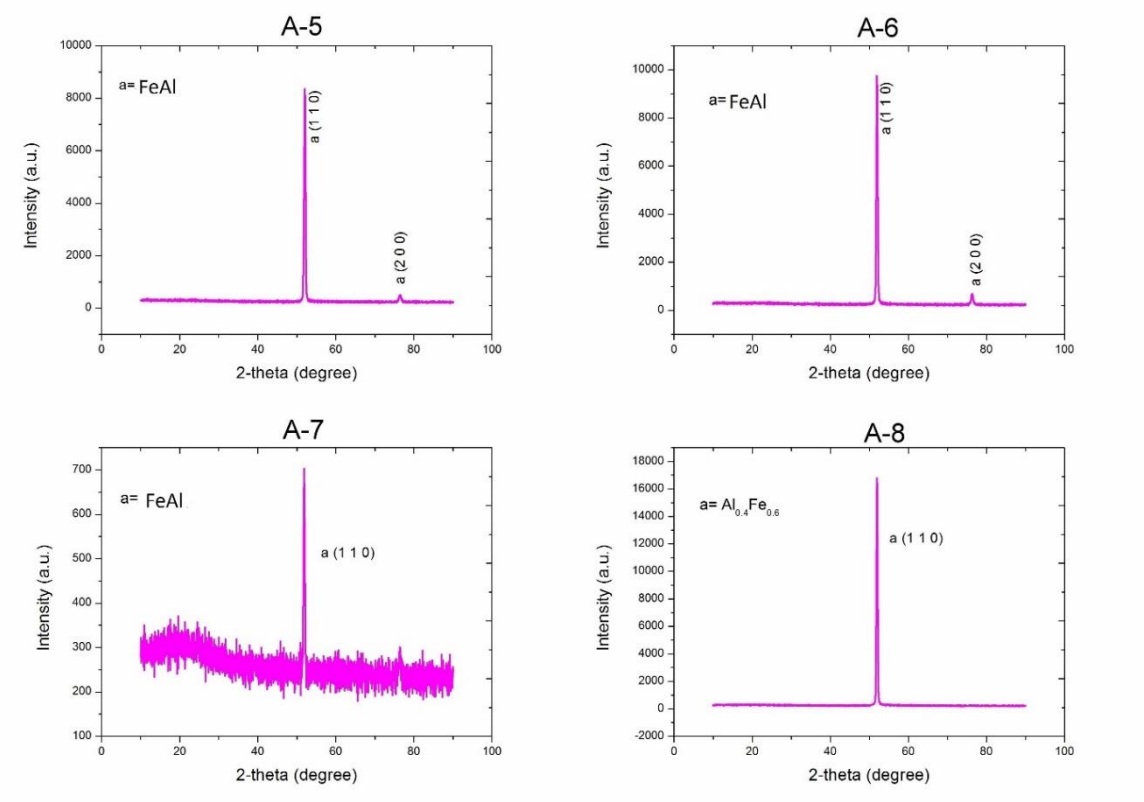

Fig 4.3(c): X-Ray Diffraction analysis of the heat treated samples after testing in Acid rain

From the Figure 4.3(b) we have seen that various intermetallic phases are present in the sample. After testing these samples in acid rain sample some intermetallic phases like $Al_{13}Fe_4$, Fe_3Al and Al_2Fe have been disappeared which has been illustrated from the figure 4.3 (c) but FeAl intermetallic phases remained as it was in the previous heat treated sample. This is showing that FeAl intermetallic phase has more corrosion resistance against acid rain.

4.3.4 XRD analysis of Sea Water Sample:

Table 3: Description of the samples name that were used in sea water treatment

Sample Name	Description of Sample
S-1	Heat Treated at 600^oC
S-2	Heat Treated at 750^oC
S-3	Heat Treated at 950^oC
S-4	Heat Treated at 1100^oC

From the Figure 4.3(b) we have seen that various intermetallic phases are present in the sample. After testing these samples in sea water some intermetallic phases like $Al_{13}Fe_4$, Fe_3Al and Al_2Fe have been disappeared which has been illustrated from the figure 4.3 (d) but FeAl

intermetallic phase remained as it was present in the previous heat treated sample. This is showing that FeAl intermetallic phase has more corrosion resistance against sea water. But the sample which was heat treated at 1100^{o}C, had no FeAl intermetallic phase hence it has least resistance to corrosion. From the figure 4.3 (d), XRD analysis of S-4 sample showed that it has formed phase with the cations and anions present in the sea water. This due to the absence of FeAl phase which is excellent against corrosion of sea water.

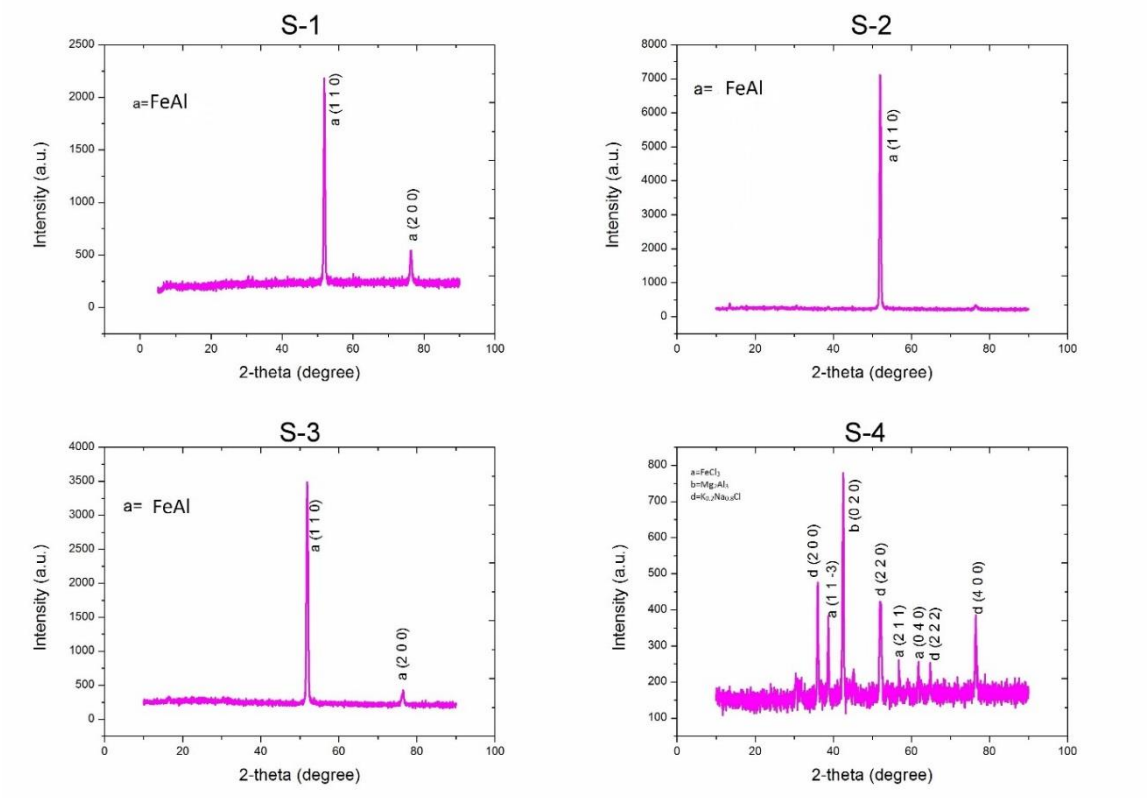

Fig 4.3(d): X-Ray Diffraction analysis of the heat treated samples after testing in Sea water

4.4 Micro hardness of the heat treated sample:

From the figure 4.4, we can depict that variation in heat treatment temperature there is variation in hardness of this Fe-Al sample. This is because of the change in phases after heat treatment, which is clearly visible from the XRD analysis of the heat treatment samples.

From the literature review, it was found that the phases like FeAl, Fe_3Al, C_3Fe_7 and $Fe_3Al_1C_1$ have more hardness value than the phases like Al_2Fe, Al_6Fe and $Fe_{13}Al_4$. The hardness of the sample which was heat treated at 1100^{o}C has the least hardness among the other heat treated samples because it has only one phase that is Al_6Fe, other than Fe, which is the

common principal element in other samples. And the sample heat treated at 950°C has the highest hardness because of the presence of the phases like FeAl, C_3Fe_7, $C_1Al_1Fe_3$ etc.

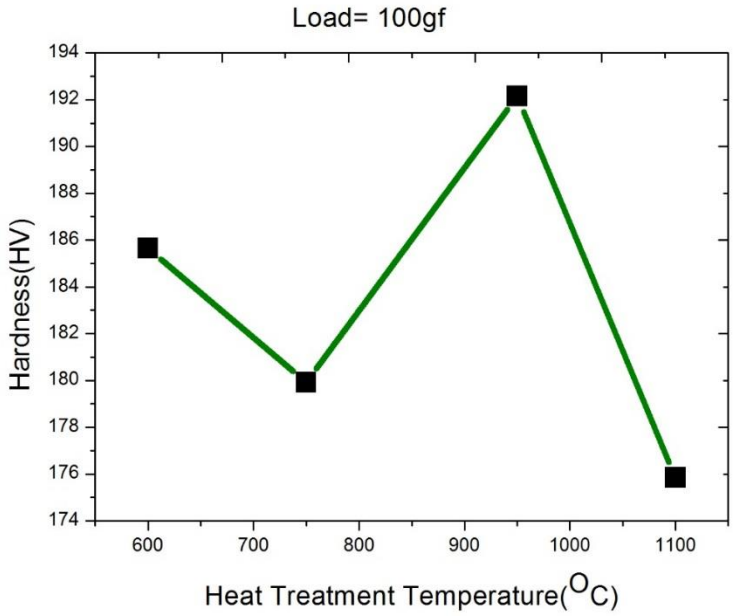

Fig 4.4: Vickers hardness graph of heat treated samples

4.5 Weight Measurement

4.5.1 Weight Measurement of Acid Rain Sample:

From the figure 4.5 (a) we can observe that the graphs are of decreasing trend in nature. But there is fluctuation in the decreasing trend, this was due to the difference in the phases that was present after heat treatment. After testing the sample in acid rain the phases like $Al_{13}Fe_4$, Fe_3Al, Al_6Fe and Al_2Fe were disappeared and FeAl the only phase that remained as it was present in the heat treated specimen.

From the figure 4.5 (a) graphs of the specimen A-5, A-6, A-7 showed that initially there was decrease in weight but after some time it was becoming constant or the decrease in weight reduced. This was due to the presence of the remained phase FeAl, which has corrosion resistance. Graph of the A-8 specimen showed that the weight is constantly decreasing this was due to the absence of FeAl phase.

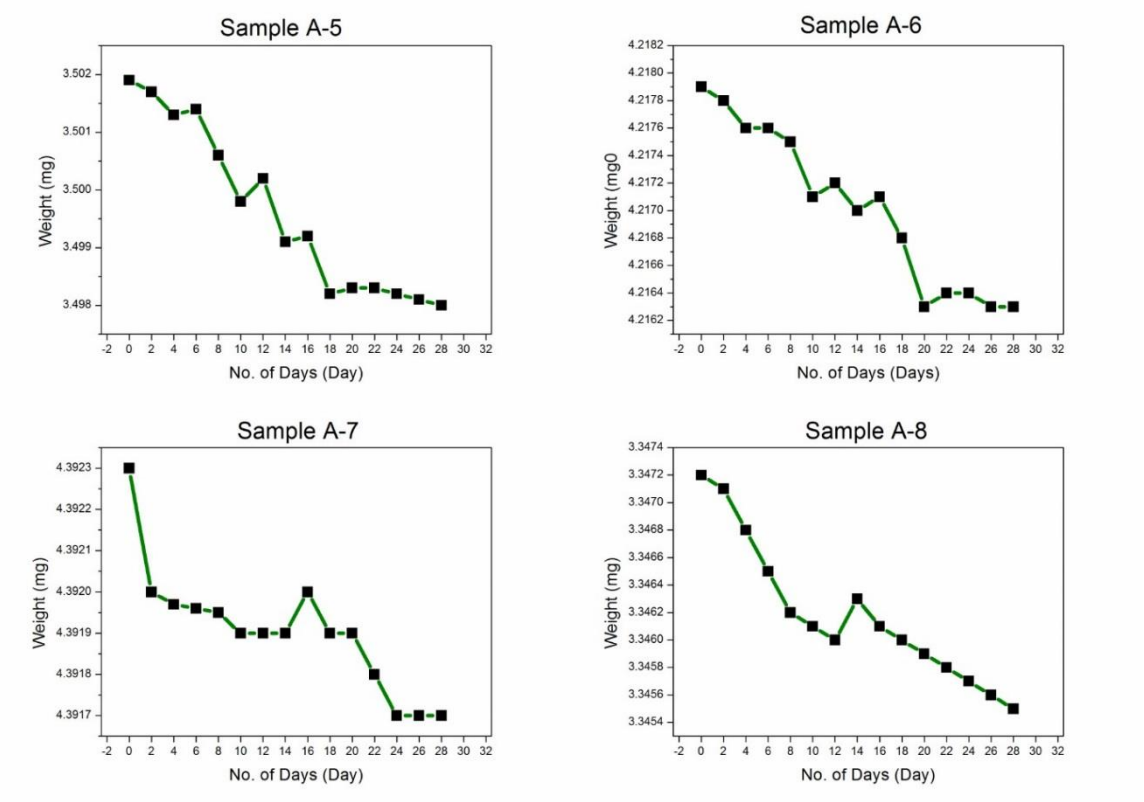

Fig 4.5(a) Weight measurement of heat treated sample in acid rain

4.5.2 Weight Measurement of Sea Water Sample:

From the figure 4.5 (b) we can observe that the graphs are of decreasing trend in nature. But there is fluctuation in the decreasing trend, this was due to the difference in the phases that was present after heat treatment. After testing the sample in sea water the phases like $Al_{13}Fe_4$, Fe_3Al, Al_6Fe and Al_2Fe were disappeared and FeAl the only phase that remained as it was present in the heat treated specimen.

From the figure 4.5 (b) graphs of the specimen S-1, S-2, S-3 showed that initially there was decrease in weight but after some time it was becoming constant or the decrease in weight reduced. This was due to the presence of the remained phase FeAl, which has good corrosion resistance. Graph of the S-4 specimen showed that there is some decrease in weight and then it also became constant, though it has no FeAl phase. This was due to the extra phase formation due to the presence of cations and anions in sea water.

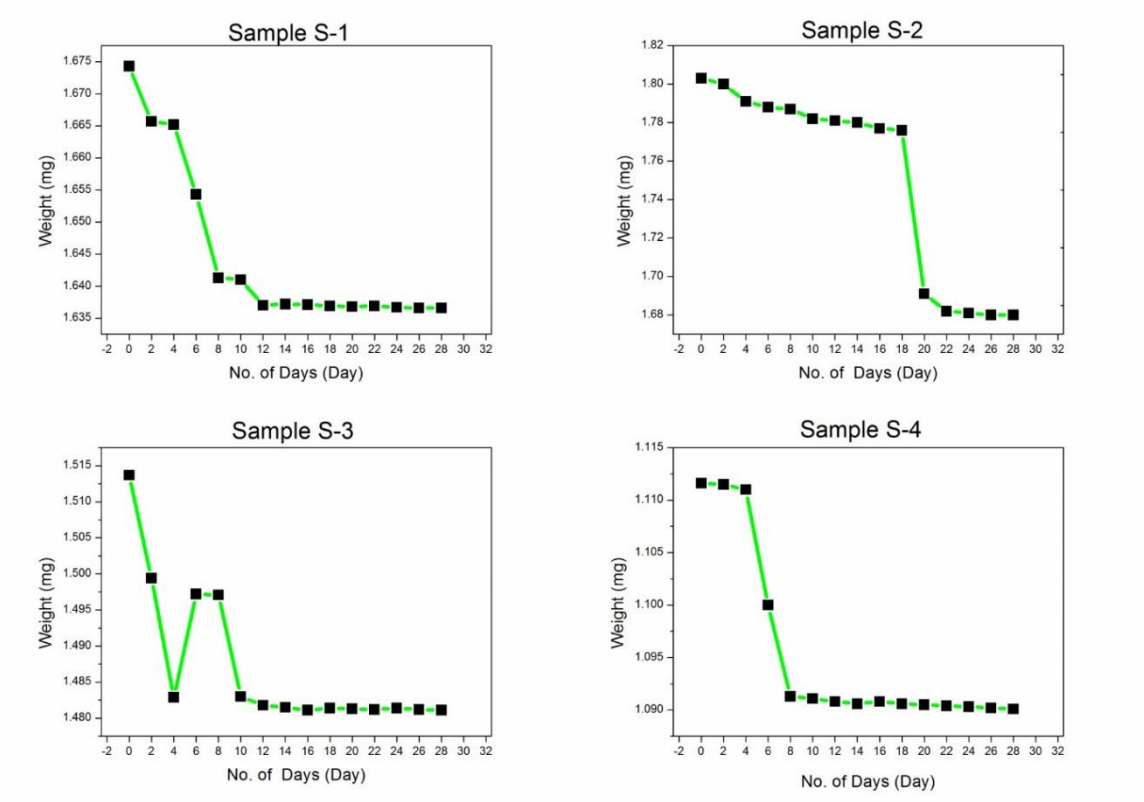

Fig 4.5(b) Weight measurement of heat treated sample in sea water

4.6 Dry Sliding Wear Test:

From the figure 4.6 (a) we can conclude that with increase in sliding distance the wear depth of the samples which were heat treated at 600^{o}C and 950^{o}C becomes stable after some initial sudden hike in depth. But the samples which were heat treated at 750^{o}C and 1100^{o}C had showed continuous increase in depth with in the same parameters. Hence this outcome strengthened our hardness result. The samples which were heat treated at 600^{o}C and 950^{o}C had more hardness value than the samples which were heat treated at 750^{o}C and 1100^{o}C.

From the figure 4.6 (a) we can infer that sample which was heat treated at 950^{o}C has the highest value of frictional force hence it has highest resistive force for indentation. Which means that it has more hardness than other samples which again strengthened our hardness results. And the sample which was heat treated at 1100^{o}C showed least value of frictional force hence it has less hardness as well as less resistive force against indentation.

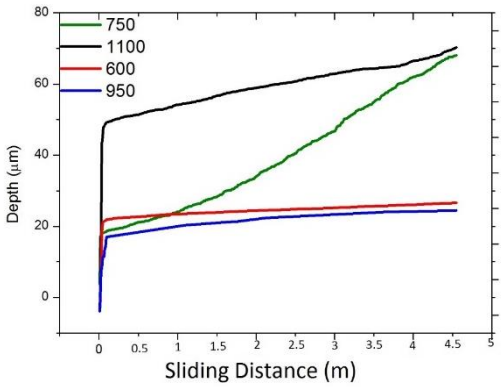

Fig 4.6: Graph of sliding distance vs wear depth

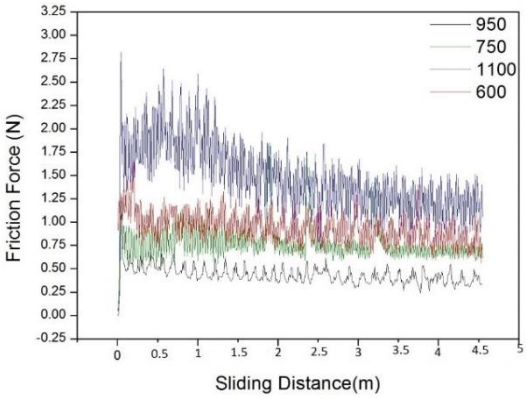

Fig 4.7: Graph of sliding distance vs friction force

4.6.1 Wear Track Width Measurement:

Sample Name in the SEM image	Heat treatment temperature (°C)	Wear Track Value (µm)
1	600	356
2	750	286
3	950	328
4	1100	390

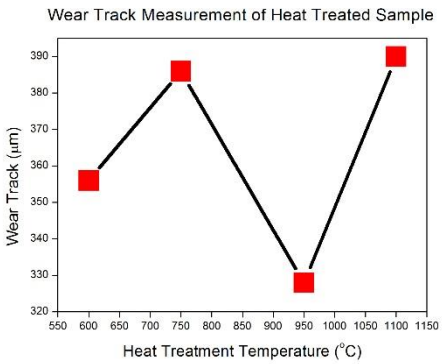

Fig 4.8: Shows the wear track values and graphical representation of these values

From the figure 4.8 it can be visualized that, the sample which was heat treated at 950°C has the least value of wear track this is due to the high hardness value which has already been shown above. And the sample which was heat treated at 750°C has the highest value of wear track because it has least hardness value. Hence we can conclude that wear track is directly proportional to hardness of the material.

The following figures are representing the wear track values during the dry sliding wear test of the teat treated samples. The description of the samples numbering are given with reference to fig 4.8

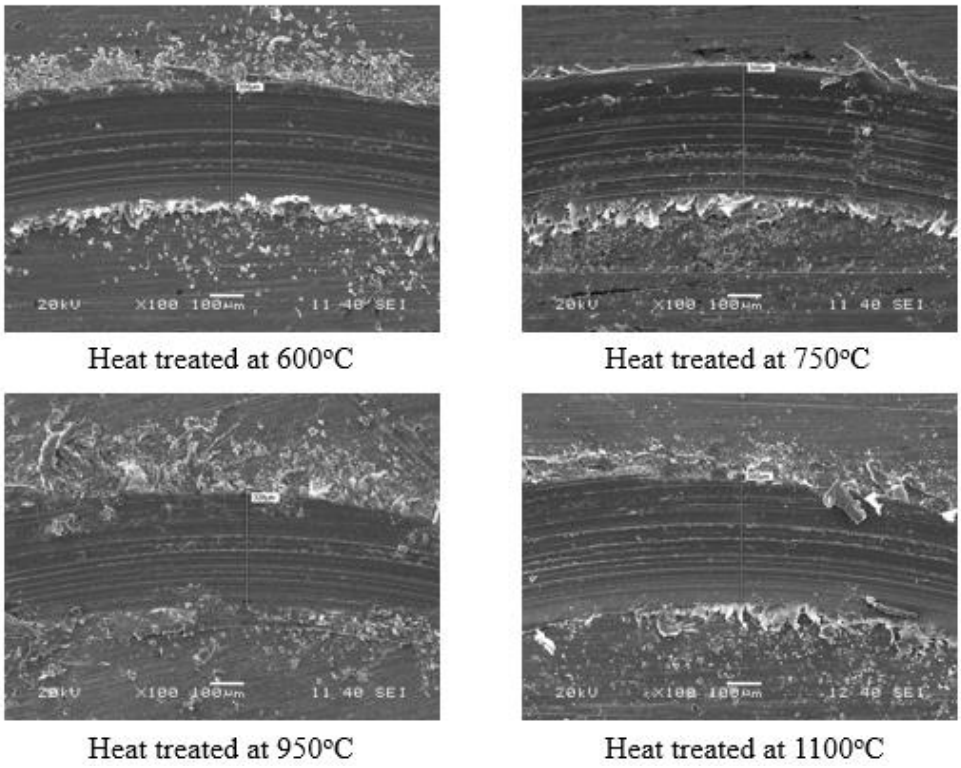

Fig 4.9: Representing the wear track width of the heat treated sample

4.6.2 Worn Surface Study:

The following SEM images of the worn surfaces are representing the wear mechanism during the dry sliding wear test of the heat treated samples. The description of the samples numbering are give with reference to the figure 4.8.

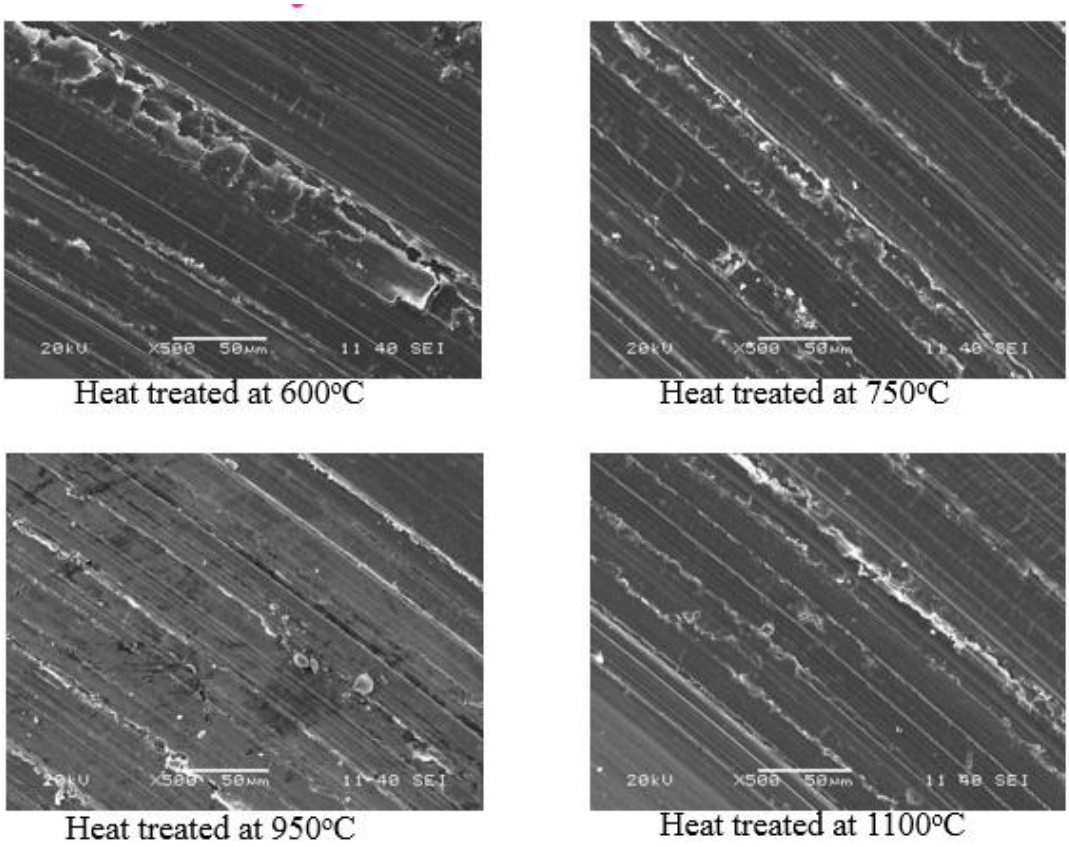

Fig 4.10: Represents the SEM of worn surface of the heat treated sample

From the figure 4.9, it is observed that the heat treated sample at 750°C and 1100°C showed mainly ploughing grooves. Hence this observation showed that the sliding wear occoured by plastic deformation as well as these two samples did not show any sharply delineated cleavage faces or the cracks of brittle nature on the wear surface. The sample which was heat treated at 600°C showed ploughing at initial stage, but with the increase in sliding distance the wear mechanism changed to microcutting. Here the observation showed that dual mode of wear mechanism was present. It may be due to the temperature increase during the wear testing period or due to the variation in phases. The sample which was heat treated at 950°C showed microcutting wear mechanism.

4.6.3 Study of the Chip formed during wear mechanism:

The following figures are representing the chip formation during the dry sliding wear test of the teat treated samples. The description of the samples numbering are give with reference to figure 4.8

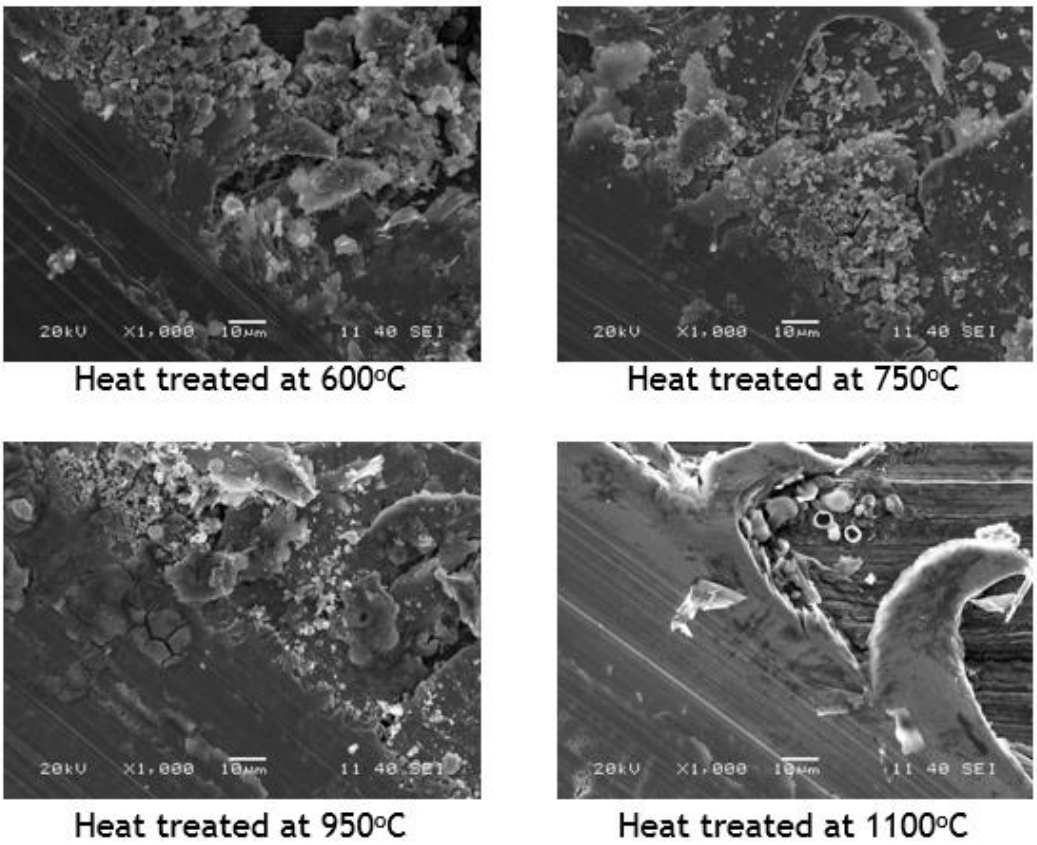

Fig 4.11: Represents the SEM images of the chip formation during the dry sliding wear test of the heat treated samples

From the figure 4.10, it can be illustrated that the sample which was heat treated at 600^{o}C has continous chip formation as well as discontinous chip formation hence it is a mixed type of material in which both ductile and brittle phases are present. But brittle phase is dominant because it has more discontinous chips than continous chips. The sample which was heat treated at 750^{o}C has shown the reverse of the 600^{o}C heat treated sample. Here it has more continous chips than discontinous chips. Hence it has more ductile phases than brittle phases. The sample which was heat treated at 950^{o}C has shown only fractures surfac as well as less discontinous chip. Hence it has all the brittle phases. The sample which was heat treated as 1100^{o}C has only continous type of chips hence it has all ductile phases.

CHAPTER - V

CONCLUSION

Conclusions:

From this piece of research work, following conclusions can be drawn. That:

- From the DSC test we found that some reaction is taking place between the temperature range and from the TG test, there is increase in mass may be due to oxidation after 1150^{o}C.
- From microstructure images of the pre heat treated hot rolled sample as well as post heat treated samples have polygonal grain structure. Due to heat treatment there were significant change in grain structure and arrangement of grains is observed.
- From X-Ray Diffraction analysis of the pre heat treated hot rolled Fe-Al alloy and post heat treated samples, formation and presence of different phases are prominent.
- The heat treated samples were subjected to acid rain and sea water treatment for corrosion testing purpose. XRD analysis of all these samples showed the presence of FeAl phase implies the highest corrosion resistance of this phase.
- The heat treated samples were subjected to Ball-on-plate tribometer for dry sliding wear test. From the results of this test we found that the samples which were heat treated at 750^{o}C and 1100^{o}C have shown a continuous increase of wear with increase in sliding distance. And also offered low resistance to the dry sliding wear. The sample which was heat treated at 950^{o}C has showed the highest resistive force against dry-sliding wear test. SEM images of the worn surfaces of these samples showed that ploughing and micro cutting were the major mechanism involved here. SEM images of the chip formation of these samples showed that the material which was heat treated at 600^{o}C showed mixed type chip formation, heat treated at 950^{o}C sample showed discontinuous type chip formation and the samples heat treated at 750^{o}C, 1100^{o}C showed mostly continuous type chip formation.
- The Vickers hardness test of these samples showed that the sample which was heat treated at 950^{o}C has the highest hardness and the sample which was heat treated at 1100^{o}C showed the least hardness.

REFERENCES

References:

[1] Palm, Martin. "Concepts derived from phase diagram studies for the strengthening of Fe–Al based alloys." *Intermetallics* 13.12 (2005): 1286-1295.

[2] S.L Case, K.R Van Horn "Aluminium in iron and steel". Chapter 1,

[3] S.L Case, K.R Van Horn "Aluminium in iron and steel". Chapter 2

[4] S.L Case, K.R Van Horn "Aluminium in iron and steel". Chapter 8

[5] S.L Case, K.R Van Horn "Aluminium in iron and steel". Chapter 10

[6] S.L Case, K.R Van Horn "Aluminium in iron and steel". Chapter 14

[7] E.B. Stong and Aston, "Wrought Iron and Its Manufacture" Byer Co. (1939)

[8] Hosford, William F. "*Iron and steel"*. Cambridge University Press, 2012, pp. 1-8

[9] Sykes, C., and J. W. Bampfylde. "The physical properties of iron–aluminium alloys." *J Iron Steel Inst* 130 (1934): 389-410.

[10] J.E. McClellan and H. Dorn, Science and Technology, World History, John Hopkins University Press, 1999, USA

[11] D. Dowson, History of Tribology, 2nd Edition, Professional Engineering Publishing, 1998.

[12] M. Eguchi and T. Yamamoto, Dynamic behaviour of a slider under various tangential loading conditions, Proc. JSLE. Int. Tribology Conference, 8-10 July 1985, Tokyo, Japan, Elsevier, 1986, pp. 1047-1052

[13] B. Bhusan, J.N. Israelachvili and U.V. Landman, Nanotribology: Friction, wear and lubrication at the atomic scale, Nature, Vol. 374, 1995, pp. 607-616.

[14] H. Yoshizawa, Y-L. Chen and J. Israelachvili, Recent advances in molecular level understanding of adhesion, friction and lubrication, wear, vol. 168, 1993, pp. 161-166.

[15] C.M. Mate, G.M. McClelland, R. Erlandsson and S. Ching, Atomic – Scale friction of tungsten tip on a graphite surface, phys. Rev. Lett., Vol. 59, 1987, pp. 1942-1945.

[16] R.J.A. van der Oetelaar and C.F.J. Flipse, Atomic-scale friction on diamond (111) studied by ultra-high vaccum atomic force microscopy, surf. Sci., vol. 384, 1997, pp. L828-835.

[17] G. Binnig and H. Rohrer, The scanning Tunnelling Microscope, Scientific American, August 1985, pp. 40-46.

[18] D.A. Bonnell, Scanning Tunnelling Microscopy and Spectroscopy, VCH Weinheim, 1993

[19] J. Krim, Friction at the atomic scale, Scientific American, Vol. 275, 1996, pp. 74-82

[20] Q. Xu, X-D. Xiao, D. Charych, F. Wolf, P. Frantz, D.F. Ogletree, Y.R. Shen and M. Salmeron, Nonlinear optical studies of monomolecular films under pressure, phys. Rev.. B, Vol. 51, 1995, pp. 7456-7463

[21] J.A. Harrison, S.J. Stuart and D.W. Brenner, Atomic-Scale Simulation of Tribological and Related Phenomena, Handbook of Micro/Nanotribology, editor: B. Bhusan, CRC Press, Boca Raton, FL,1998.

[22] C.G McKamey, J.H Devan, P.F Tortorelli, V.K Sikka, J. Mater. Res. 6(1991) 1779-1805.

[23] D.G. Morris, M.A. Morris-Muñoz, The influence of microstructure on the ductility of iron aluminides, Intermetallic 7 (1999)1121–1129.

[24] S. Frangini, N. DeCristofaro, J. Lascovich, A. Mignone, Corros. Sci. 35 (1993) 153-159.

[25] S. Frangini, N. DeCristofaro, A. Mignone, J. Lascovich, R. Giorgi, Corros. Sci. 39 (1997) 1431-1442.

[26] D. Schaepers, H.H Strehblow, Corros. Sci. 39 (1997) 2193-2213

[27] X. Guan, K.Iwasaki, K. Kishi, M. Yamamoto, R. Tanaka, Dry sliding wear behaviour of Fe–28Al and Fe–28Al–10Ti alloys, Mater.Sci.Eng.:A366 (2004) 127–134.

[28] X. Zhang, J. Ma, L. Fu, S. Zhu, F.Li, J. Yang, W.Liu, High temperature wear resistance of Fe–28Al–5Cr alloy and its composites reinforced by TiC, Tribol. Int. 61(2013)48–55.

[29] G. Sharma, P.K. Limaye, R.V. Ramanujan, M. Sundararaman, N.Prabhu, Dry- sliding wear studies of Fe3Al-ordered intermetallic alloy, MaterSci.Eng.:A 386 (2004)408–414

[30] Y.-S. Kim, Y.-H. Kim, Sliding wear behaviour of Fe3Al-based alloys, Mater. Sci. Eng.: A258 (1998) 319 –3 24.

[31] E.G Zakahrova, Deformation mechanics and strain hardening of Hadfield steel single crystals alloyed with aluminium, Doklady physics 47 (7) (2002) 515-517

[32] M. Abbasi, Sh. Kheirandish, Y. Kharrazi, J. Hejazi, "The fracture and plastic deformation of aluminium alloyed Hadfield steels", Materials Science and Engineering A 513-514 (2009) 72-76

[33] B.K Zuidema, D.K Subramanyam, W.C Leslie, "The effect of aluminium on the work hardening and wear resistance of Hadfield manganese steel", Metallurgical Transaction A 18A (1987) 1629-1639

[34] Ren, Jiangwei, and Dong Li. "Fine surface microstructure of Fe 3 Al alloy after severe plastic deformation." *Materials Letters* 171 (2016): 133-136.

[35] Hasemann, G., et al. "Vacancy strengthening in Fe 3 Al iron aluminides."*Intermetallics* 54 (2014): 95-103.

[36] Sharma, Garima, et al. "Dry-sliding wear studies of Fe 3 Al-ordered intermetallic alloy." *Materials Science and Engineering: A* 386.1 (2004): 408-414.

[37] Kim, Yong-Suk, and Yong-Hwan Kim. "Sliding wear behavior of Fe 3 Al-based alloys." *Materials Science and Engineering: A* 258.1 (1998): 319-324.